Structure, Volume *26*

Supplemental Information

The Amaryllidaceae Alkaloid Haemanthamine Binds the Eukaryotic Ribosome to Repress Cancer Cell Growth

Simone Pellegrino, Mélanie Meyer, Christiane Zorbas, Soumaya A. Bouchta, Kritika Saraf, Stephen C. Pelly, Gulnara Yusupova, Antonio Evidente, Véronique Mathieu, Alexander Kornienko, Denis L.J. Lafontaine, and Marat Yusupov

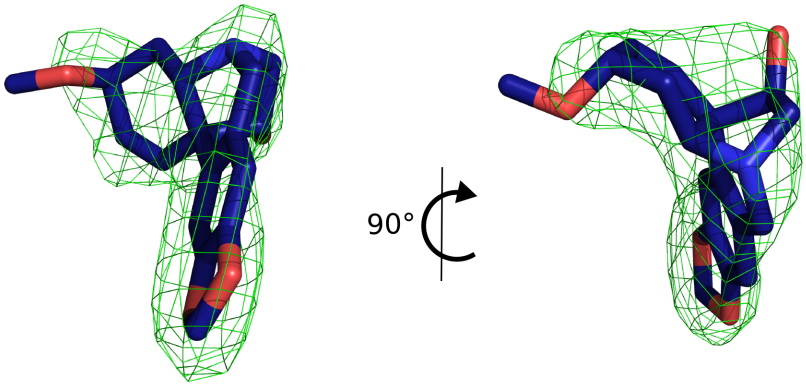

Figure S1: Density quality allow us to unambiguously determine HAE position and binding mode. Related to Figure 2. Unbiased F_{obs} - F_{calc} electron density map issue of the first cycle of rigid-body refinement using the vacant *S. cerevisiae* 80S structure (PDB ID: 4V88) as starting model. The map (represented as green meshes) includes only the HAE compound, it is contoured at 3σ and is represented in two views, 90° apart.

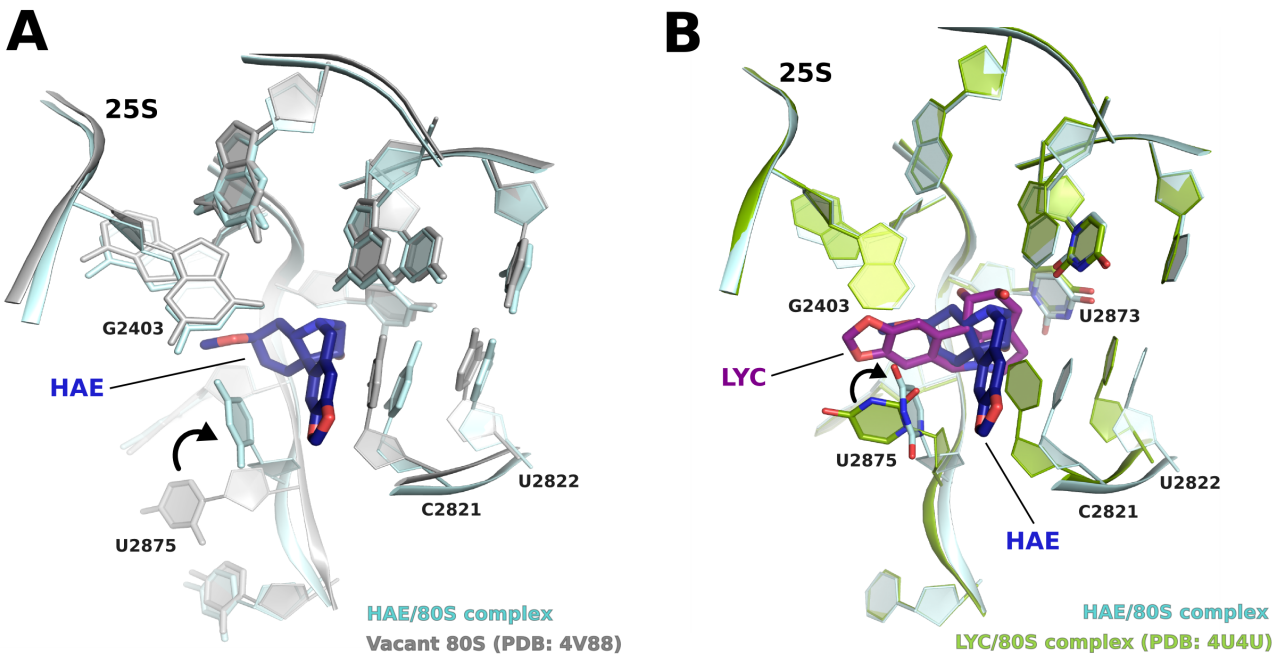

Figure S2: Rearrangement of the A-site cleft on the 25S rRNA is inhibitor dependent. Related to Figure 3. (A) Superposition of the A-site cleft of vacant yeast 80S ribosome (PDB ID: 4V88) with our structure. We can observe that residues C2821 and U2822 are displaced upon accommodation of the inhibitor, likely driven by hydrophobic forces that push them away from the PTC, as seen in the case of NAR/80S structure (PDB ID: 4U51). The "flip-up" movement of residue U2875, not observed for other alkaloids before, is significant and likely induces further stabilization of the HAE in the A-site cleft. (B) Superposition based on the LSU of the HAE/80S A-site cleft (this work) with the LYC/80S complex previously published (PDB code: 4U4U). Although the binding pocket is constituted by the same residues and the compounds share chemical structure similarity, the interactions network is remarkably different.

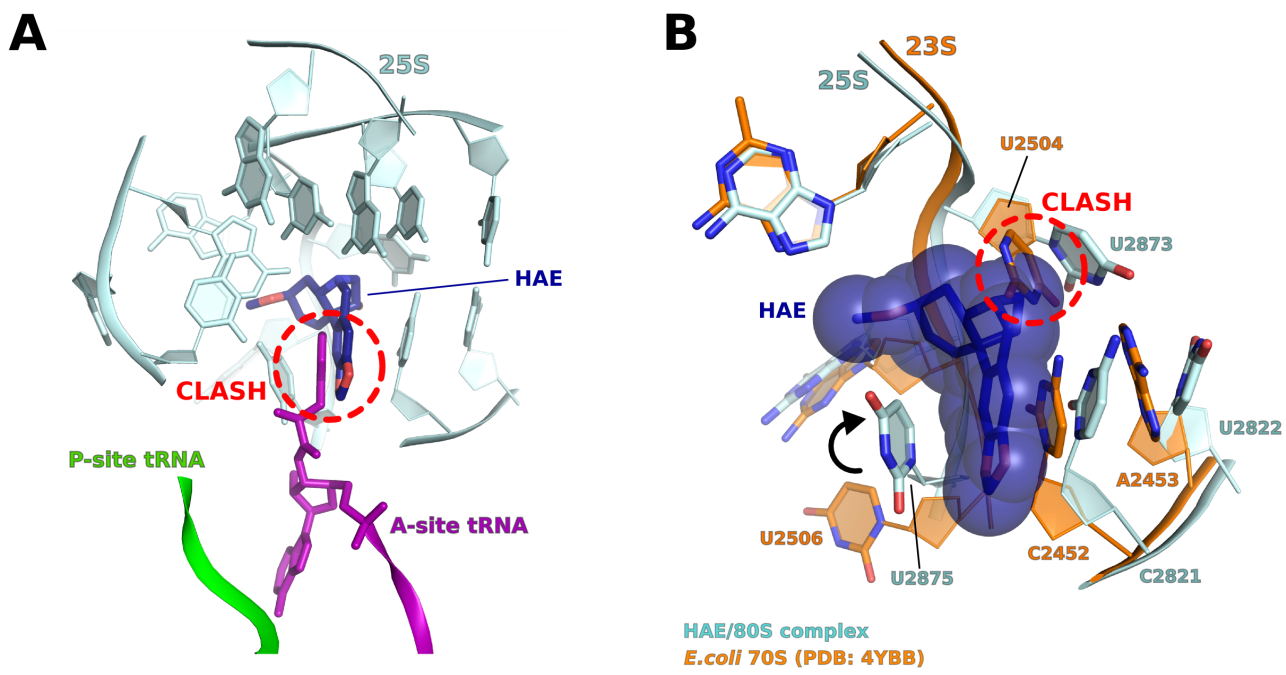

Figure S3: HAE is an eukaryotic specific inhibitor and its binding is predicted to clash with the newly coming A-site tRNA. Related to Figure 3. (A) *In silico* model of an actively translating 80S ribosome. Aminoacylated A- and P-site (amino acid not shown for clarity) tRNAs are taken from the 70S structure of *T. thermophilus* (PDB ID: 4V5D), after superposition of the *S. cerevisiae* 25S rRNA with the bacterial 23S rRNA. The steric clash that would occur upon HAE binding to the A-site cleft is highlighted in red. HAE will impair the accommodation of any long-chain or bulky amino acid in the A-site cleft, thus blocking the elongation phase of translation. (B) Superposition of the 25S rRNA A-site cleft of the HAE/80S complex with the *E. coli* vacant 23S rRNA structure (PDB ID: 4YBB). We can observe several rearrangements of the rRNA residues in the pocket. Although some displacements are very similar to what has been detected in the vacant *S. cerevisiae* 80S structure (Fig. S2A), precisely concerning the movement of the C2452 and U2506 (C2821 and U2875 in yeast, respectively), the analysis pinpoints the likely candidate in charge of discriminate the inhibitor's binding between the two kingdoms. The residue U2504 (U2873 in yeast) is adopting a different conformation in the bacterial A-site cleft, as a consequence of the presence of a purine (instead of a pyrimidine) close to the conserved C2452 (C2821 in yeast). The conformation of U2504 would then sterically clash with the inhibitor, likely rejecting its binding to the pocket and making it inefficient for interaction with the bacterial ribosome.

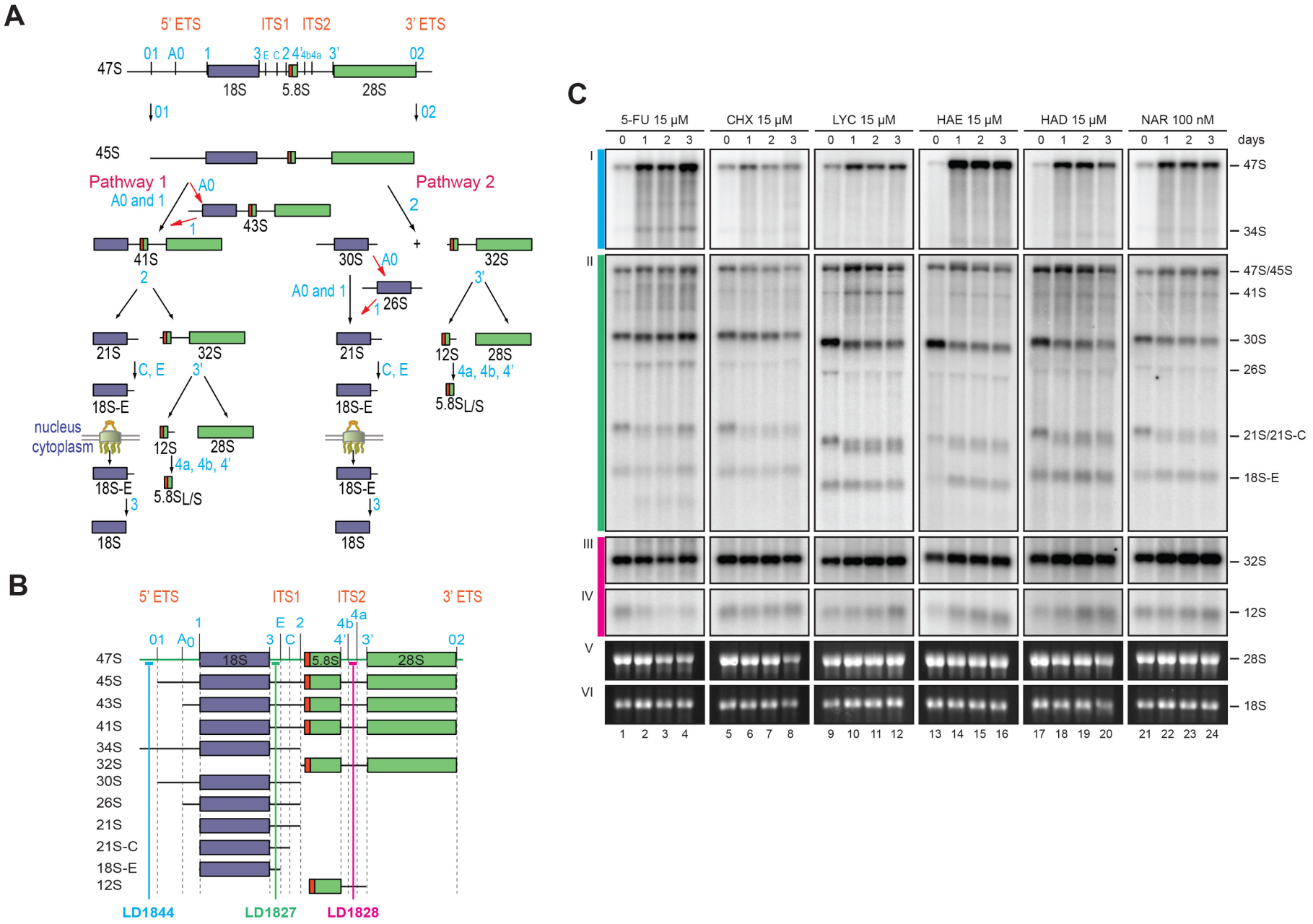
A
5' ETS
ITS1
ITS2
3' ETS
01
A0
1
3
E
C
2
4'
4b
4a
3'
02
47S
18S
5.8S
28S
45S
Pathway 1
A0 and 1
Pathway 2
43S
41S
30S
32S
26S
21S
C, E
3'
18S-E
12S
28S
4a, 4b, 4'
5.8S L/S
nucleus
cytoplasm
18S
B
LD1844
LD1827
LD1828
21S-C
C
5-FU 15 µM
CHX 15 µM
LYC 15 µM
HAE 15 µM
HAD 15 µM
NAR 100 nM
days
I
II
III
IV
V
VI
47S
34S
47S/45S
41S
30S
26S
21S/21S-C
18S-E
32S
12S
28S
18S

Figure S4: Effects of *Amaryllidaceae* alkaloids on pre-rRNA processing in cultured cancer cells. Related to Figure 6. (A) Pre-rRNA processing pathway in human cells and major pre-rRNA intermediates (see Mullineux and Lafontaine, 2012 for details). Three of the four mature rRNAs, the 18S, 5.8S, and 28S rRNAs are produced from a single RNA Pol I transcript (47S). The 18S rRNA is the RNA component of the small subunit (40S); 5.8S and 28S are incorporated into the large subunit (LSU, 60S). There is a third rRNA in the 60S subunit, 5S, which is independently produced by RNA Pol III (not shown). The mature sequences are embedded in noncoding 5' and 3' external transcribed spacers (ETS) and internal transcribed spacers (ITS1 and 2). Cleavage sites (in cyan) and alternative pathways are indicated (pathways 1 and 2). For details, see Www.RibosomeSynthesis.Com. (B) Northern blot probes used in this work (LD1844, LD1827, and LD1828) highlighting the pre-rRNA species detected. (C) Northern blot analysis. Total RNA extracted from HCT116 cells treated with the indicated *Amaryllidaceae* alkaloid for 1, 2, or 3 days was resolved on denaturing gels and analyzed by Northern blotting with specific probes (see panel B). As controls, cells were treated with 5-FU or CHX. Remarkably, the pre-rRNA processing inhibitions observed with the four AAs are highly similar (e.g. 32S accumulation and 21S/21S-C and 18S-E accumulation only seen in AA-treated cells). Furthermore, the AA processing inhibitions are highly specific as they are strikingly different to those observed with the control compounds (5-FU and CHX: reduced 32S and no effect on 32S, respectively, and no particular effects on 21S/21S-C or 18S-E). Blots were probed with oligonucleotide LD1844 (panel I), LD1827 (panel II), or LD1828 (panels III and IV). Panels V and VI show ethidium-bromide-stained gels.

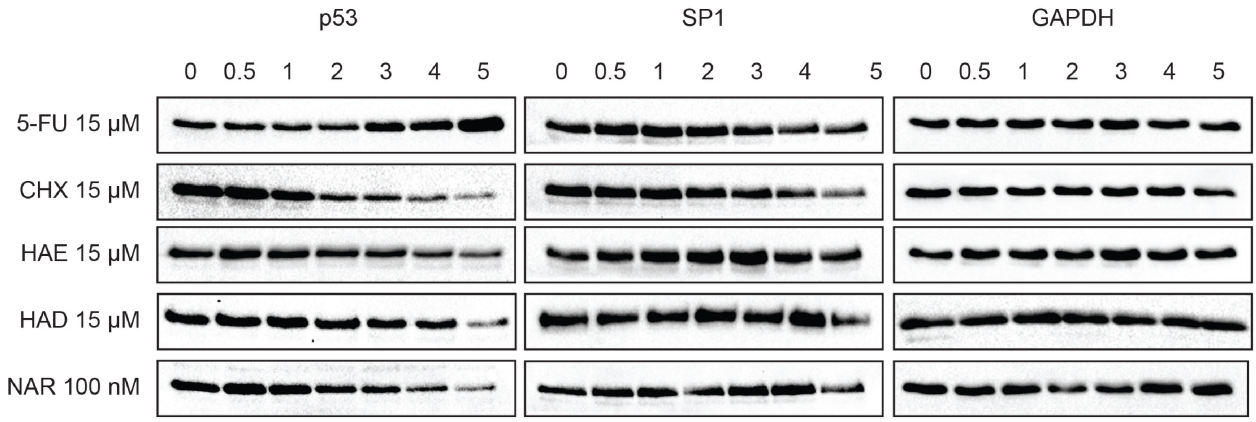

Figure S5: Effects of *Amaryllidaceae* alkaloids on p53 homeostasis. Related to Figure 6. Analysis of p53 steady-state accumulation. The figure shows the same samples as those presented in Fig. 6B with the blots probed for additional loading controls (SP1 and GAPDH). Total protein was extracted from HCT116 cells treated with the indicated compound in a time-course analysis for up to 5 hours and analysed by Western blotting. The blots were probed with an antibody specific to p53, SP1, or GAPDH (control).

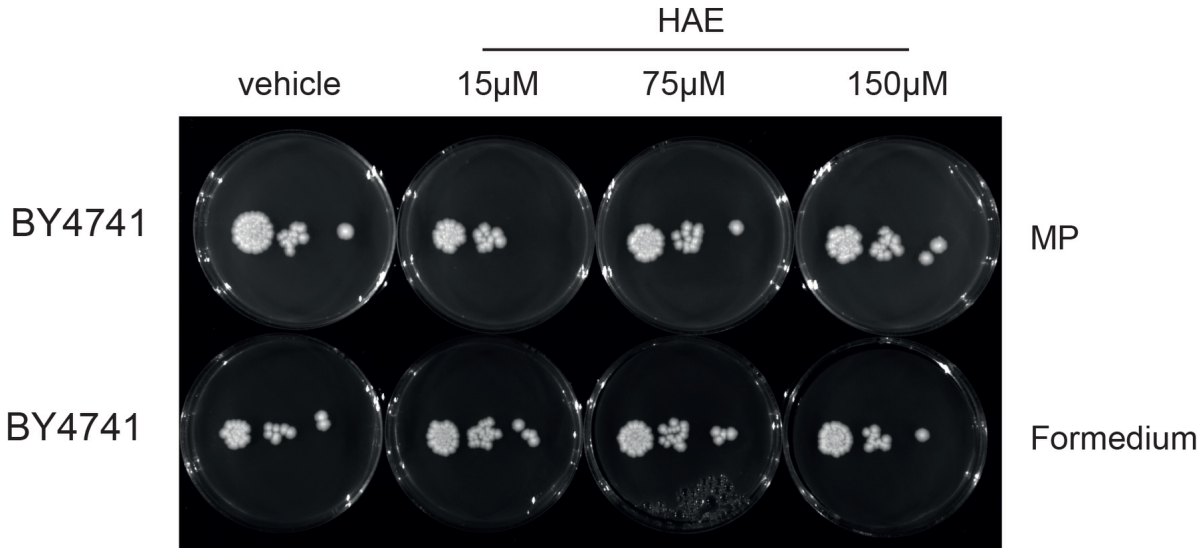

Figure S6: Yeast cells are not sensitive to haemanthamine. Related to Figure 6. The data show that yeast cells are not sensitive to HAE even at concentration 10 times higher than those used on human cells. The wild-type strain used is the Euroscarf consortium wild-type BY4741. From left to right: vehicle alone (DMSO 0.15%), HAE 15 μM, HAE 75 μM, and HAE 150 μM. The complete medium was prepared with yeast extracts from two suppliers as we previously observed that yeast extract origin may influence drug sensitivity. Top raw: yeast extract from MP; bottom raw: yeast extract from Formedium (STAR Methods). The results are the same with both yeast extracts.

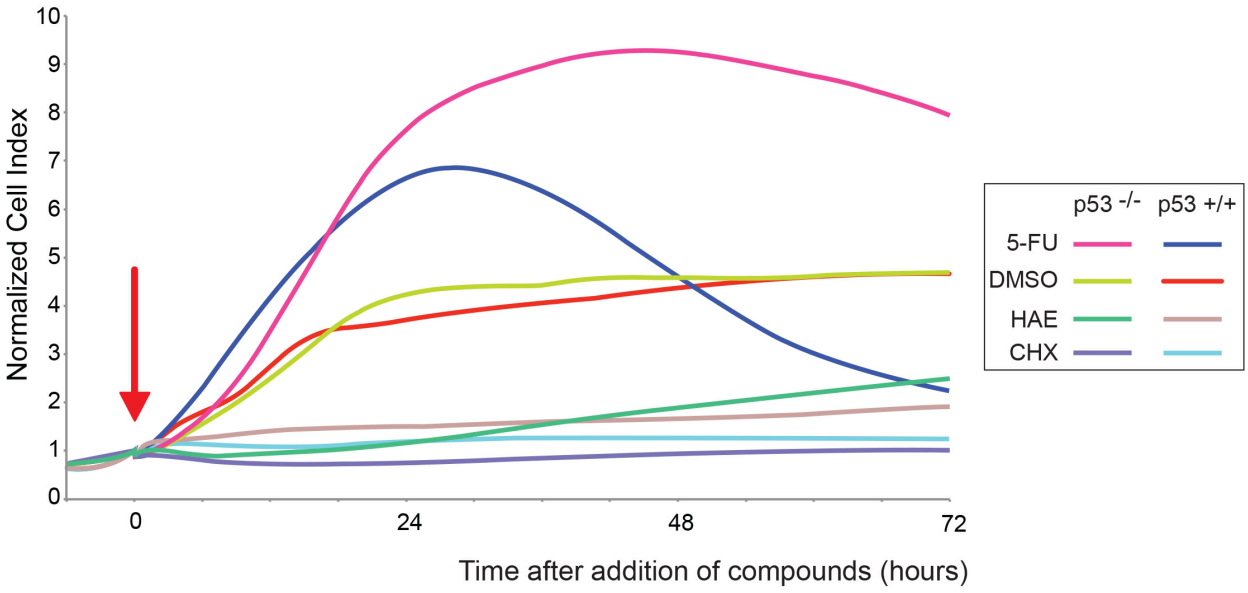

Figure S7: The effects on cancer cell proliferation of compounds that activate nucleolar stress (5-FU and HAE) require the presence of p53 in cells. Related to Figure 6. Two isogenic diploid human cancer cell lines, one expressing p53 (HCT116 p53 +/+) and one not expressing p53 (HCT116 p53 -/-), were seeded on gold-plated multi-well plates, treated with the indicated compounds, and cell proliferation monitored by real-time impedance measurements for 3 days. The growth of cells treated with 5-FU declines more rapidly and more sharply in cells that express p53 (navy blue profile) than in cells that do not express p53 (in pink). Similarly, the cell growth is more inhibited upon HAE treatment in cells that express p53 (in brown) than in cells that do not express p53 (dark green). In contrast, treatment of cells with CHX, which does not activate nucleolar stress, inhibits growth similarly in presence (cyan) or absence (purple) of p53 (i.e. parallel profiles). As control, cells treated with the drug vehicle alone (DMSO) grow similarly irrespective of their p53 status: the light green and red profiles are similar (red, HCT116 p53 +/+; light green, HCT116 p53 -/-). All compounds were used at 15 μM and added after 1 day of growth (0-hr time point, red arrow). The results are expressed as normalized cell index. The experiment was performed in duplicate, the mean is shown.